CONF-790815--5

GA-A15475

MASTER

DESIGN OF ALUMINUM STABILIZED SUPERCONDUCTOR FOR TOKAMAK TOROIDAL FIELD COILS

by

W. Y. CHEN, J. S. ALCORN, and J. R. PURCELL

JUNE 1979

GENERAL ATOMIC COMPANY

DISCLAIMER

GA-A15475

DESIGN OF ALUMINUM STABILIZED SUPERCONDUCTOR FOR TOKAMAK TOROIDAL FIELD COILS

by

W. Y. CHEN, J. S. ALCORN, and J. R. PURCELL

This is a preprint of a paper to be presented at the 1979 International Cryogenic Materials Conference, Madison, Wisconsin, August 21-24, 1979.

Work supported by
Department of Energy
Contract DE-AT03-76ET51011

GENERAL ATOMIC PROJECT 3235.869.001

JUNE 1979

GENERAL ATOMIC COMPANY

DESIGN OF ALUMINUM STABILIZED SUPERCONDUCTOR FOR TOKAMAK TOROIDAL FIELD COILS*

W. Y. Chen, J. S. Alcorn and J. R. Purcell
General Atomic Company, San Diego, California

INTRODUCTION

High purity aluminum has superior stabilization performance than copper for high field (10 - 12 T) applications due to the low electrical resistivity of pure Al, and the fact that the magneto-resistivity of pure Al saturates above ≈6 T. Stabilization with pure Al becomes increasingly attractive as the peak field is increased. The resistivity of pure Al is about five times lower than Cu under similar cyclic stress and neutron irradiation conditions expected for a tokamak toroidal field (TF) coil environment. Based on the overall economics of the reactor, it is highly desirable to utilize pure Al as the stabilizer so that the radial extent of the TF-coils can be reduced through reduction in the required stabilizer area; however, due to the extremely poor mechanical properties of pure Al which has a yield strength of about 8.3 MPa (1200 psi), special attention must be paid in the conductor design so that the pure Al stabilizer is properly supported, and most of the electromagnetic and mechanical forces are transmitted through the reinforcement material. The volume occupied by the reinforcement material partially offsets the advantage gained through Al stabilization.

A design study has been carried out on an Al-stabilized 10 - 12 T TF-coil cooled with pool boiling LHe. Relevant factors considered include the mechanical properties of pure aluminum, the degradation in resistivity due to neutron

*Work supported by Department of Energy, Contract DE-AT03-76ET51011.

irradiation, the selection and configuration of the reinforcement materials, and the overall stability of the conductor. Both alloy Al and stainless steel has been considered as the reinforcement material. Special attention has been paid to ensure sufficient cooling of the conductor. The goal of the study is to generate a design which can be compared directly with the design of a Cu-stabilized TF-coil.

RELEVANT PROPERTIES OF HIGH PURITY ALUMINUM

The electrical resistivity of high purity aluminum is of the most interest among the various properties. Figure 1 is a plot of the resistivity of pure aluminum as a function of the ambient field strength [1]. Also plotted in Fig. 1 are the resistivity curves of pure aluminum when stressed to 0.1% and 0.2% elongation, and when cyclically stressed after 1000 cycles at elongations of 0.1% and 0.2%, and also the resistivity of OFHC Cu (RRR ≈ 200). It can be seen that even with the severe cyclic stressing applied ($\varepsilon = 0.2\%$ at 1000 cycles), pure aluminum still has a lower resistivity than unstressed OFHC Cu in the field region of interest. The margin is between 2 to 5, and is improving with increasing field strength.

One significant advantage of pure aluminum is that its magneto-resistivity saturates at fields above 6 T, in comparison, the magneto-resistivity of Cu increases steadily with field. Thus at high field pure aluminum is expected to offer much better stabilizing performance.

The change in resistivity of pure aluminum under neutron irradiation is another property of concern. Pure aluminum is more susceptible to irradiation damage than copper. Based on the information in Ref. [2], for a dose of

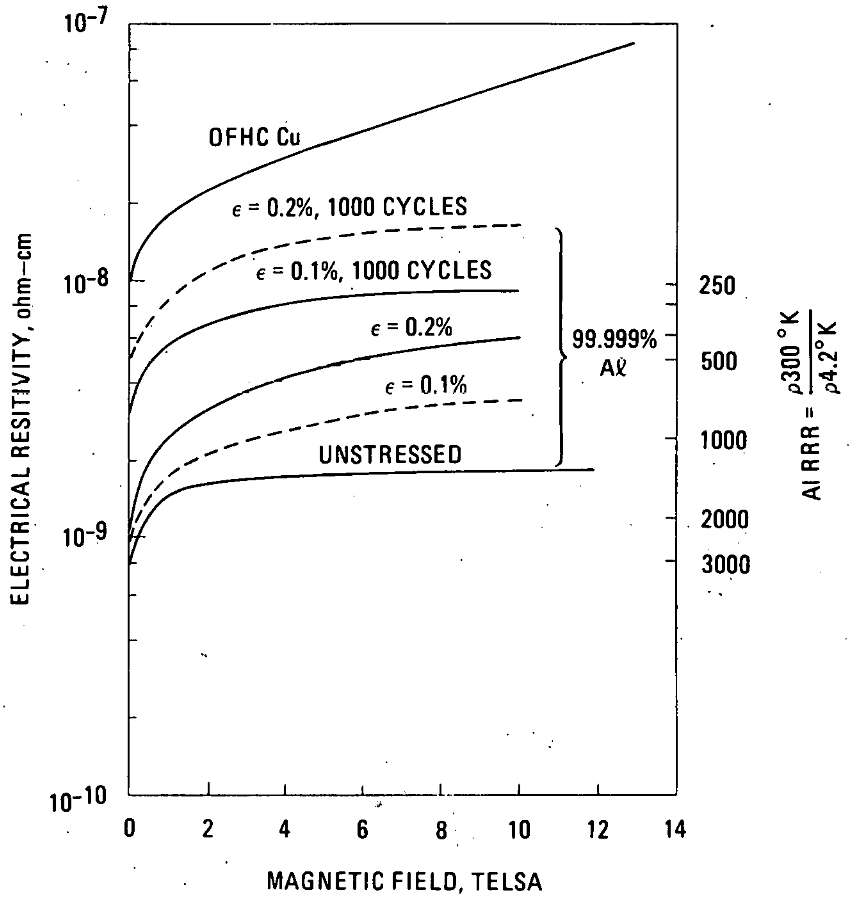

Fig. 1. Electrical resistivity versus magnetic field (4.2 K). Dotted lines are projected values [1].

8×10^{16} n/cm^2 which causes the resistivity in Cu to increase by 0.38×10^{-8} Ω-cm (about 20% of the initial value), the increase in resistivity for pure aluminum is 1.3×10^{-8} Ω-cm. The amount of increase $\Delta\rho$ is almost proportional to the dose.

Figure 2 is a plot of the thermal-conductivities of pure aluminum and OFHC Cu as a function of temperature [1]. It can be seen that pure aluminum also has higher thermal-conductivity than OFHC Cu at low temperature, and therefore offers better stabilization through the enhanced ability to conduct heat away from a normal zone.

The poor mechanical properties of pure aluminum presents a problem in utilizing it as a stabilizing material. The yield strength of pure aluminum

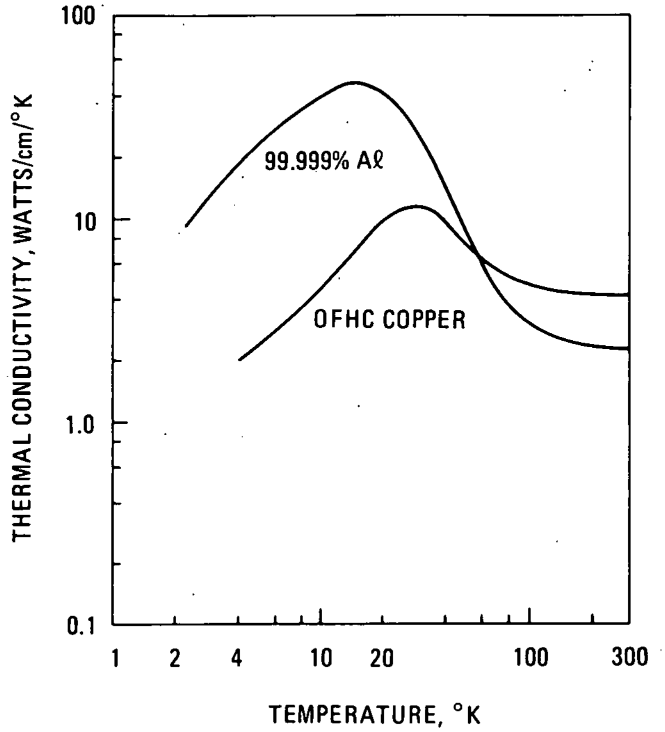

Fig. 2. Thermal conductivity versus temperature

at 4.2 K is merely 8.3 MPa (1200 psi), which is far lower than the typical level of stress in a TF-coil ($\gtrsim$ 69 MPa or 10,000 psi). Conductors made of pure aluminum behave essentially as fluid under such high stress levels unless the applied forces are properly transmitted to a reinforcement material. The problem can also be solved by properly encasing the pure aluminum in a sealed structure made with high strength material.

DESIGN CONSIDERATIONS

The high field TF-coil conductor must be designed to withstand bearing pressures as high as 70 MPa. Furthermore, the tensile load typically 70 MPa in magnitude in the winding must be carried either by the conductor itself or by a separate reinforcement component. For an Al-stabilized conductor, a separate reinforcement material must be used to withstand both the bearing load and the tensile load to prevent the pure Al from deformation due to forces applied on the conductor. Two possible schemes of reinforcement are:

1. As shown in Fig. 3-A, which is the cross sectional view of the conductor, the reinforcement material is placed on three of the four faces of the conductor. The two side walls are made thick so that when the conductors are stacked up in the winding, the bearing forces are transmitted through the side walls, and the pure aluminum does not experience the bearing forces. On the unreinforced face, pure aluminum is exposed, and indentations can be made on the side walls so that coolant can reach the pure aluminum for direct cooling, although such a channel is limited in coolant content. Indentations on the side walls can be made large enough so that a portion of the sides of the pure Al stabalizer is available for cooling. The tensile load can be taken by a separate stainless steel strip, but it is also possible to combine the reinforcement components into a single structure so that the conductor module is reinforced against both the tensile and bearing loads.

2. As shown in Fig. 3-B, this configuration utilizes the reinforcement material to encase the pure aluminum and NbTi completely. The reinforcement materials acts as the wall of a pressure vessel, with the pure Al being the pressurized fluid. This configuration allows the bearing forces to be transmitted even through the pure Al, and may lead to a design requiring less reinforcement material in the conductor, and therefore relatively thin walls. Then the side walls are available for cooling as long as the conductance of the side

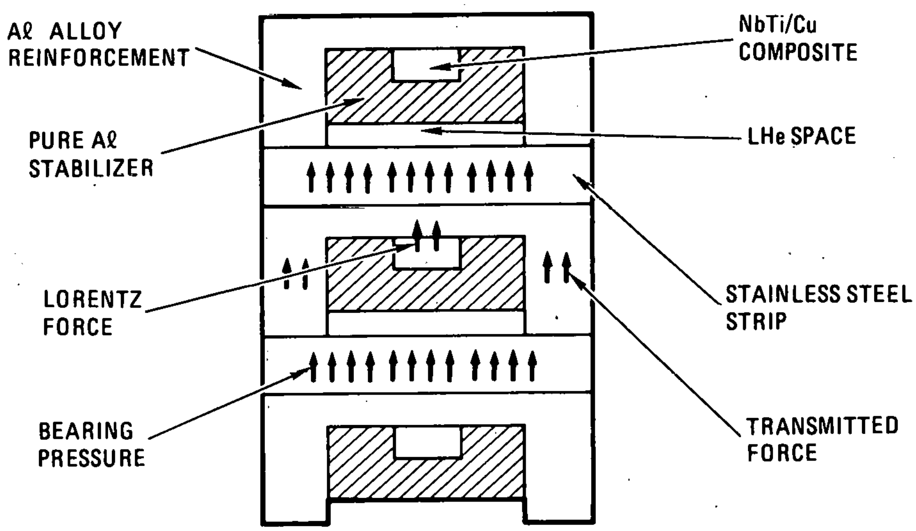

(A) REINFORCED SIDE-WALLS (RSW)

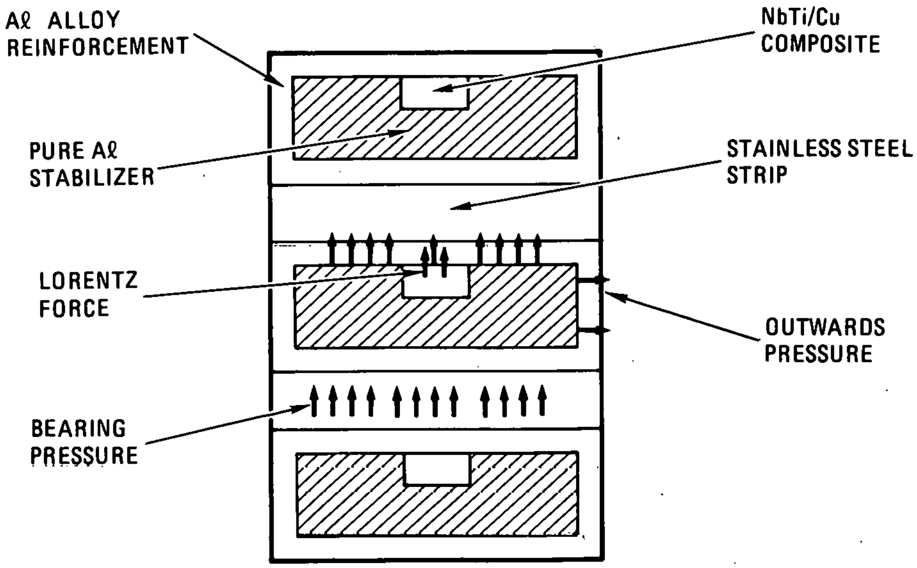

(B) COMPLETE ENCASING (CE)

Fig. 3. Two possible schemes of reinforcing the pure Al. Also shown are the manner in which the bearing forces are transmitted through the conductors.

wall is low so that only a small temperature gradient is generated. Even portions of the force-bearing faces are available for cooling if indentations are formed on the faces. The complete encasing also offers better overall mechanical protection to the pure Al. The tensile load in the winding is best taken with separate stainless steel strips in this approach.

The selection of the reinforcement is another important issue. The material must have good mechanical properties (high yield stress and ultimate stress), temperature coefficients compatible to Al, and reasonable thermal conductivity. High strength aluminum alloys such as the 2024 class or the 6061 class appear to be well suited for the application. For the reinforced side wall approach, it is desirable to utilize stainless steel as much as possible due to its superior mechanical strength.

DESIGN DESCRIPTION

The 10 T TF-coil being studied is for a 3.6 m TNS device [3]. A corresponding TF-coil design based on Cu-stabilized conductor has been carried out by General Atomic [3,4]. Table I lists the various relevant parameters. Except for the conductor modules, the overall coil design and fabrication scheme of the Al-stabilized version is nearly identical to the design of the Cu-stabilized version [3,4].

The peak field considered was 12 T. However, conductors for the 10 - 12 T field region were considered separately because the 12 T coil is designed to operate with 2 K LHe bath cooling rather than the 4 K bath cooling used in the 10 T version.

Table I. Design Parameters of Al-Stabilized TF-Coil (10 T Version)

Plasma major radius (m)	3.6
On-axis field (T)	5.0
Number of coils	12
Peak field (T)	10.0
Total ampere turns (A-T)	90×10^6
Coolant	Pool boiling LHe at 4.2 K
Superconductor	NbTi
Stabilizer	High purity Al
Reinforcement materials	Stainless steel Aluminum alloy
Insulation materials	Mylar and fiberglass epoxy
Outer radius of centerpost winding (m)	1.80
Total tensile force/coil (Newtons)	58.3×10^6

Conductors based on both the reinforced side wall (RSW) concept and the complete encasing (CE) concept have been considered. In the RSW conductor, stainless steel was used as the only reinforcement material, whereas in the CE conductor, encasing was made with alloy Al, while a separate stainless steel strip was used to withstand the tensile load. Figure 4-A and 4-B are sketches of the two types of conductors.

Both types of conductor employ similar types of superconducting core/stabilizer. The core of the conductor is a multi-filamentary NbTi-Cu composite fabricated in the conventional manner. The amount of Cu is kept low since it is not used for stabilization. The NbTi-Cu composite is metallurgically bonded to the pure Al stabilizer, and then the entire structure is either encased in the Al-alloy casing in the CE scheme, or is embedded into the stainless steel structural support in the RSW scheme.

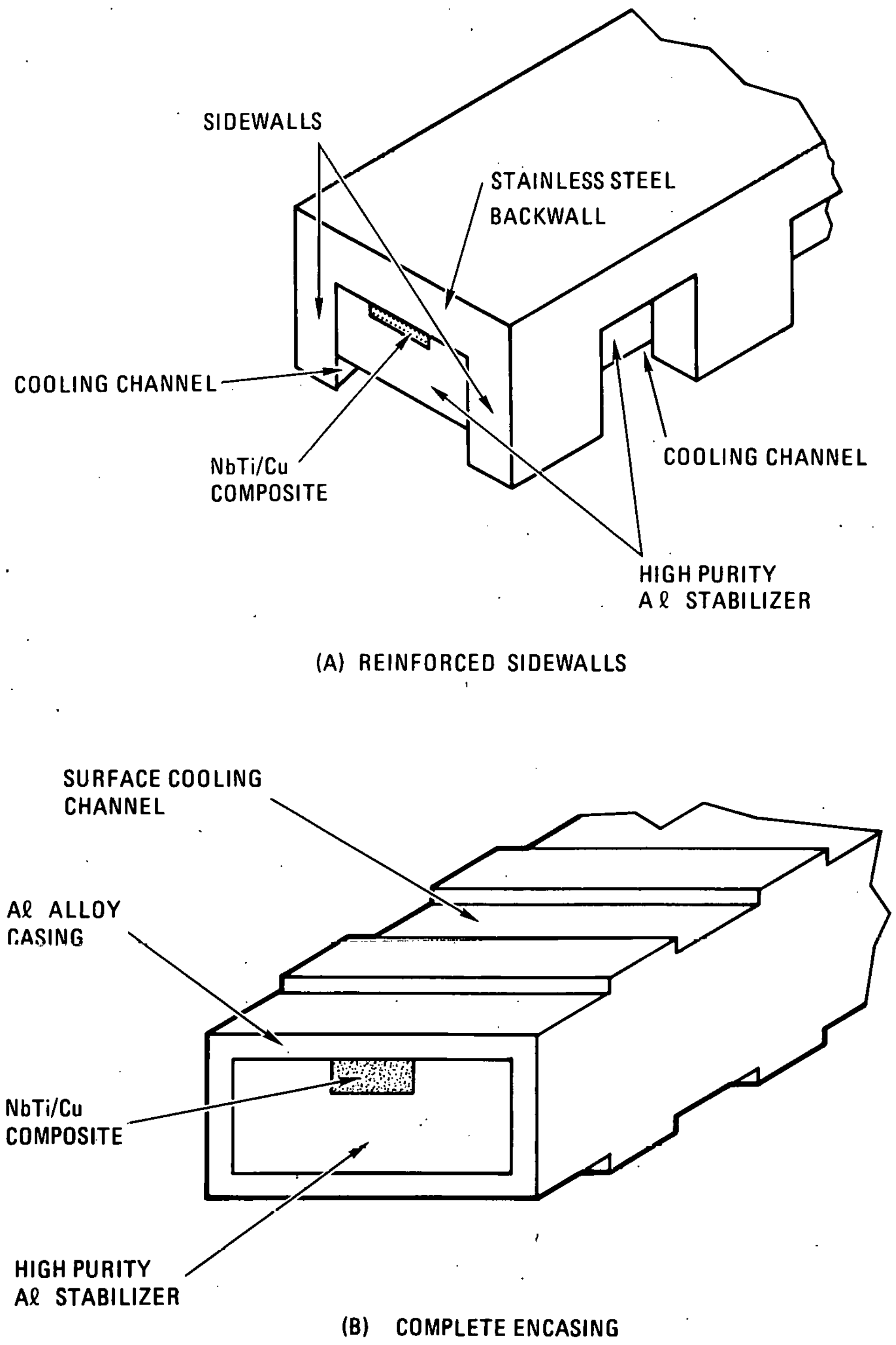

Fig. 4. Sketch of the two conductor configurations adopted in the design study

The amount of pure Al in the conductors for each field region is determined according to the stability criterion described below. The conductors are designed to recover from a disturbance represented by a 1 meter long normal zone with initial temperature of 20 K. The behavior of the conductors was studied by numerical simulation of the evolution of the initial normal zone [5]. The effect of the low thermal-conductivity of the Al-alloy conductor casing was considered in the simulation.

The mechanical aspects of the designs for the two types of conductors are:

1. In the RSW scheme the thickness of the reinforcement side wall is determined from the bearing pressure. The maximum tolerable stress of stainless steel was taken to be 550 MPa (~80,000 psi). The stress in the side wall was in general much lower than the buckling stress, or the shearing stress at the joint between the side wall and the back wall. The thickness of the back wall was determined from the tensile load.

2. In the EC scheme the thickness of the alloy Al casing was determined so that it can contain the pressure transmitted from the bearing faces through the fluidic pure Al to the side walls. The alloy Al is also used to contain part of the tensile load. The stainless steel strips are used as the primary containment of the tensile forces. During winding, the SST strips are used for prestressing the alloy Al to widen the range the alloy Al can be stressed.

RESULTS AND DISCUSSION

The dimensions and parameters of the conductor for each field region are summarized in Table II for both RSW and EC schemes. It can be seen that the radial extents of each field region are close, with the RSW design giving rise to slightly smaller radial extent at low and medium field.

Table II. Summary of Conductor/Module Dimensions and Parameters for each Field Region in the 10 T Version

Field Region	9 - 10 T	7 - 9 T	5 - 7 T	3 - 5 T	0 - 3 T
Al resistivity 10^{-8} Ω-cm	2.8	2.15	1.50	1.40	1.40
J_c of NbTi A/cm^2	10^4	4×10^4	8×10^4	1.15×10^5	1.15×10^5
Pure Al area, (cm^2)					
RSW	1.61	1.82	0.97	0.97	1.07
CE	1.13	1.58	1.04	0.93	0.95
Casing thickness (cm) CE	0.09	0.10	0.12	0.132	0.143
Sidewall thickness (cm) RSW	0.2	0.2	0.3	0.3	0.4
Alloy Al area (cm) CE	0.70	0.71	0.78	0.84	0.81
Stainless steel thickness (cm) CE	0.5	0.5	0.5	0.5	0.5
Backwall thickness (cm) RSW	0.55	0.55	0.55	0.55	0.55
Fraction of face cooling (%) CE	75	75	75	75	50
Conductor height (cm) CE	1.30	1.00	0.75	0.70	0.70
Module height (cm)					
RSW	2.205	1.745	1.33	1.33	1.405
CE	2.05	1.75	1.64	1.59	1.59
Bearing pressure (MPa)	23.5	28.3	41.4	49.7	58.0
Number of turns/pancake	3	6	6	7	14
Radial extent of region (cm)					
RSW	6.62	10.47	7.98	9.31	19.67
CE	6.15	10.50	9.00	10.15	20.30

The design parameters of the resulting TF-coils and also some of the corresponding parameters adopted in the Cu-stabilized version [3] are summarized in Table III.

Table III. Major 10 T TF-Coil Design Parameters

	Al Version (CE)	Al Version (RSW)	Cu Version
Peak field, T	10.0	10.0	10.0
Number of conductor grades	5	5	5
Current/turn, A	10^4	10^4	10^4
Total stainless steel area/coil, cm^2	1.02×10^3	1.52×10^3	7.68×10^2
Total stabilizer area/coil, cm^2	8.16×10^2	9.13×10^2	2.03×10^3
Alloy Al area/coil, cm^2	5.76×10^2	--	--
Cooling channel area, cm^2	4.06×10^2	3.16×10^2	3.63×10^2
Total area, cm^2 (stainless steel + conductor + cooling)	2.82×10^3	2.75×10^3	3.13×10^3
Centerpost winding outer radius, cm	180	180	180
Pre-stress in SST, MPa	69.0	69.0	138.1
Conductor width, cm	2.75	2.75	2.75
Thickness of SST strip per turn, cm	0.5	--	0.32
Turn-to-turn insulation thickness, cm	0.05	0.05	0.05
Conductor face cooling channel depth, cm	0.2	0.2	0.2
Interlayer spacer/channel thickness, cm	0.25	0.25	0.25
Total radial extent of winding, cm	56.1	54.0	60.2

It can be noticed from Table III that in both Al-stabilized versions, although the total stabilizer areas are much lower (816 cm^2 for CE and 913 cm^2 for RSW) than the Cu-stabilized version (2.03×10^3 cm^2), because of the softness of pure Al, larger amounts of stainless steel (1.02×10^3 cm^2 for CE and 1.52×10^3 cm^2 for RSW) must be used to contain the tensile force compared with the Cu version (7.7×10^2 cm^2). Both Al versions require less total radial extents than the Cu version. The RSW version requires the least radial extent due to the utilization of high strength stainless steel as the only reinforcement material. In short, a 10% saving in total radial extent can be achieved by utilizing Al stabilization as compared with Cu stabilization.

For 12 T operations, the TF-coil design will be significantly different due to the necessity of operating at lower temperatures (2 K). Also, the magnetic load and bearing load on the conductor will be 40% higher, therefore more reinforcement material will be required. However, if only the 10 - 12 T field region is considered, and conductors based on Al and Cu stabilizations are designed, then a total module height per turn of 2.24 cm resulted from Cu stabilization, and 2.21 cm and 2.05 cm resulted from the RSW and CE versions, respectively, based on Al stabilization. It is expected that the complete TF-coil based on Al stabilization will have smaller radial extent than the Cu version if a detailed design effort is carried out.

CONCLUSIONS

In summary, the design study of an Al-stabilized 10 T TF-coil for the 3.6 m TNS tokamak reactor has been performed. Two different concepts for reinforcing the pure Al stabilizer have been considered. The designs can be directly compared with the design of the similar coil based on conventional Cu-stabilization. It was discovered that although the pure Al offers a much lower resistivity and better stabilization performance than Cu, due to its poor mechanical properties and therefore requiring more reinforcement material in the winding, the possible gain in savings in the winding radial extent is partially offset, resulting in a slightly smaller net radial extent for the Al designs. Due to more efficient utilization of reinforcement material, the reinforced sidewall concept resulted in a smaller radial extent compared with the complete enasing concept.

REFERENCES

1. D. A. Koop, "Design of 55,000 Ampere (7 Tesla) Aluminum/Nibium-Titanium Conductors for MHD Magnets," Alcoa Report ML 59242, October 1977.
2. G. McCracken and S. Blow, "The Shielding of Superconducting Magnets in a Fusion Reactor," Culham Laboratory Report CLM-R 120, August 1972.
3. "GA TNS Project, Status REport for FY-78," Vol. VI, General Atomic Report GA-A15100, October 1978.
4. J. Alcorn and J. R. Purcell, "General Atomic's Superconducting Toroidal Field Coil Concept," Proc. 6th Int. Conf. on Magnet Technology, Bratislava, Czechoslovakia, August 1977.
5. W. Y. Chen and J. R. Purcell, "Numerical Study of Normal Zone Evolution and Stability of Composite Superconductors," J. Appl. Phys. 49, 6, 1978.

GA INTERNAL DISTRIBUTION

Document Center
J. Alcorn
J. Beal
L. Bikadi
R. Bourque
S. Burnett
W. Chen
E. Cheng
V. Cravens
J. Dalessandro
P. Fortescue
J. Gilleland
D. Graumann
R. Hager
E. Hoffman
G. Hopkins
E. Hubbard
Y. Hsu
T. Jensen
G. Lutz
G. Melese-D'Hospital
P. Miller
R.L. Miller
T. Ohkawa
N. Ohyabu
M. Otavka
W. Parker
P. Parks
T. Petrie
F. Puhn
J. Purcell
J. Rawls
C.L. Rickard
S. Rosenwasser
P. Sager
L. Southworth
T. Tamano

EXTERNAL DISTRIBUTION

TIC (2)

Dr. Richard Aamodt, Director
Laboratory for Applied Plasma Studies
Science Applications, Inc.
P.O. Box 2351
La Jolla, California 92037

Dr. Charles C. Baker
Argonne National Laboratory
Fusion Power Program, Bldg. 208
9700 S. Cass Avenue
Argonne, Illinois 60440

Dr. John E. Baublitz
Office of Fusion Energy
Department of Energy, MSG-234
Washington, D.C. 20545

Dr. Frank Coffman
Office of Fusion Energy
Department of Energy, MSG-234
Washington, D.C. 20545

Mr. Daniel Cohn
MIT National Magnet Lab
170 Albany Street
Cambridge, Massachusetts 02139

Dr. Robert Conn
University of Wisconsin
Nuclear Engineering Department
Madison, Wisconsin 53706

Dr. N. Anne Davies
Office of Fusion Energy
Department of Energy, MSG-234
Washington, D.C. 20545

Dr. John M. Dawson
University of California
Department of Physics
Los Angeles, California 90024

Dr. T. K. Fowler
Associate Director for CTR
Lawrence Livermore Laboratory
P.O. Box 808
Livermore, California 94550

Dr. Melvin E. Gottlieb
Plasma Physics Laboratory
Princeton University
P.O. Box 451
Princeton, New Jersey 08540

Mr. Charles R. Head
Office of Fusion Energy
Department of Energy, MSG-234
Washington, D.C. 20545

Mr. Edwin E. Kintner, Director
Office of Fusion Energy
Department of Energy, MSG-234
Washington, D.C. 20545

Mr. Donald L. Kummer, Manager
Materials and Processes,
McDonnell-Douglas Astronautics
Company-East
St. Louis, Missouri 63166

Mr. M. Murphy
Office of Fusion Energy
Department of Energy, MSG-234
Washington, D.C. 20545

Dr. R.S. Pease --AIR MAIL--
Culham Laboratory
United Kingdom Atomic Energy Authority
Abingdon, Berkshire, England

Dr. F. Robert Scott
Electric Power Research Institute
P.O. Box 10412
Palo Alto, California 94304

Dr. Don Steiner
Oak Ridge National Laboratory
P.O. Box Y
Oak Ridge, Tennessee 37831

Dr. Clyde Taylor
Lawrence Livermore Laboratory
P.O. Box 808
Livermore, California 94550

Dr. Klaus M. Zwilsky
Office of Fusion Energy
Department of Energy, MSG-234
Washington, D.C. 20545